

Low-field Hall coefficient R_H^0 of dilute Al-3d alloys at 4.2 K

C. Papastaikoudis, D. Papadimitropoulos, and E. Rocofyllou

Nuclear Research Center "Dimocritos," Aghia Paraskevi, Athens, Greece

(Received 18 January 1980)

Measurements of the low-field Hall coefficient R_H^0 and the relative transverse magnetoresistivity $\Delta\rho/\rho_0$ of dilute solid solutions of Cr, Mn, and Fe in aluminum are presented. The results show a systematic dependence of R_H^0 on the atomic d -occupation number of the impurities. They also show that R_H^0 acquires unusually large negative values. Kesternich's three-group model is used to obtain scattering anisotropy parameters from the experimental data. The results, which suggest that the mean free paths of electrons in the corners of the second-zone Fermi surface and of those in the third zone are more nearly the same than for other dilute impurities in Al, are interpreted in terms of the simultaneous presence of a resonant scattering by the localized d states as well as a nonresonant scattering by the Coulomb potential of the impurity.

I. INTRODUCTION

The aluminum-based 3d transition-metal alloys have been studied by several authors both from the experimental and theoretical points of view. These alloys are thought to be a typical example of a system which should be analyzed with the concept of the Friedel-Anderson model of the virtual 3d bound state.^{1,2} Indeed, the change in the residual resistivity,³ thermopower,⁴ magnetic susceptibility,⁵ specific heat,⁵ and superconducting critical temperature^{6,7} can be interpreted very satisfactorily in terms of the 3d virtual bound state (VBS) moving across the Fermi level. If the position of this VBS is very near to the Fermi level of the host metal, it causes a resonant scattering of the host conduction electrons.

The main physical parameters of these Al-3d-transition-metal alloys, which have been investigated very extensively, are the electrical resistivity, thermopower, magnetic susceptibility, specific heat, and superconducting critical temperature, while very few measurements have been made of the Hall coefficient and magnetoresistance. Kedves *et al.*⁸ have measured the Hall coefficient of Al-Cr and Al-Mn alloys at 78 K. McAlister *et al.*⁹ have also measured the Hall coefficient of the same alloys at 6 and 77 K, respectively, while Papastaikoudis *et al.*¹⁰ have measured the Hall coefficient and the magnetoresistance of Al-Cu alloys at 4.2 K.

These measurements show that when Cr is added to Al the low-field coefficient R_H^0 becomes more negative, whereas the addition of Mn gives the opposite shift and the addition of Cu even gives positive values. To account for the large negative values of the low-field coefficient of Al-Cr and Al-Mn alloys, McAlister *et al.*⁹ proposed a metallurgical interpretation rather than one dealing with the nature of the 3d ions, namely that (i) dilute concentrations of Cr and Mn form an inter-

stitial phase in Al rather than a substitutional one or (ii) that the dominant scatterers in their alloys are extended clusters of solute rather than isolated ions.

The purpose of the present investigation is to examine whether the metallurgical condition of the Al-3d alloys or the presence of the virtual bound 3d state more strongly affects the low-field coefficient R_H^0 , which in the case of Al-Cr alloys⁹ is about the same as the free-electron value $-3.47 \times 10^{-5} \text{ cm}^3/\text{A s}$ of pure Al. In order to investigate more thoroughly the dependence of the low-field Hall coefficient on the atomic d -occupation number, we have extended the measurements to Al-Fe alloys. The solid solubility of transition elements in Al is very small. Thus we concentrate the measurements on samples in the dilute region, except for Al-Fe, where we have also prepared a sample above the solubility limit.

II. EXPERIMENTAL PROCEDURE

The dilute alloys of Al-Cr were produced for us from high-purity aluminum by the Instituto Sperimentale dei Metalli Leggeri, Novara, Italy, while the alloys of Al-Mn and Al-Fe were obtained from the Institut für Festkörperforschung KFA Jülich, Germany. The alloys were prepared by HF-levitation melting and then rolled into polycrystalline foils of about 100- μm thickness. The sample shapes, which were stamped out from these foils with a special steel presstool, were rectangular ($20 \times 2 \text{ mm}^2$) with two similar extensions for the magnetoresistance contacts and two other central extensions for the Hall contacts. The thickness of the specimens was determined with a conventional microscope. The error in the thickness does not exceed 4%.

After cleaning in acetone and in boiling distilled water, the samples underwent the Boato *et al.*³ treatment in order to obtain homogeneous solid

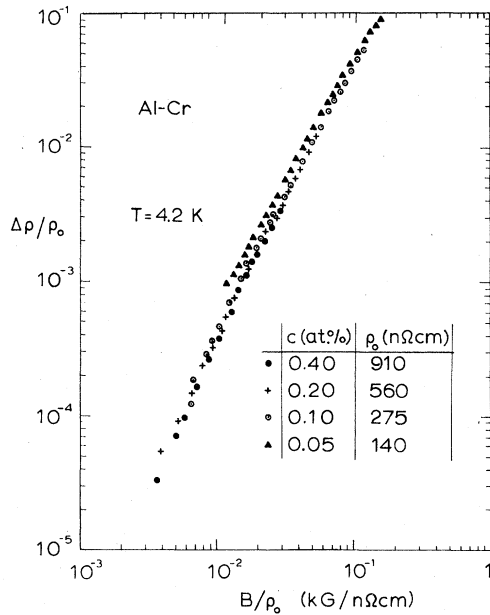


FIG. 1. Kohler diagram of the transverse magnetoresistivity $\Delta\rho/\rho_0$ for the Al-Cr alloys as a function of B/ρ_0 .

solutions whenever thermodynamically possible, namely, the specimens were annealed in air for 24 h at 640 °C—a temperature just below the nearest eutectic temperature. The samples were then quenched very rapidly in iced water and thereafter kept at room temperature. The effectiveness of the solution process was monitored by residual-resistivity measurements.

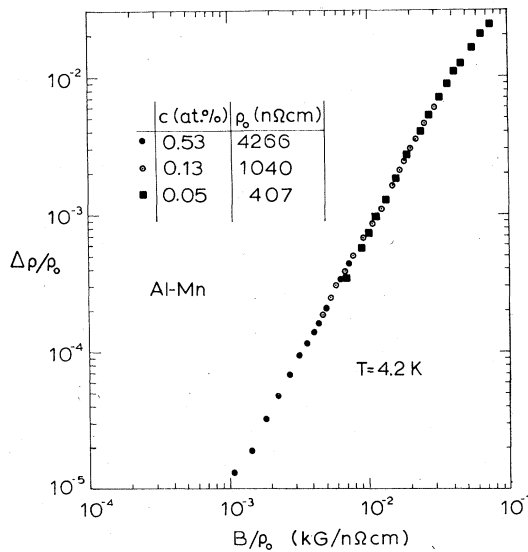


FIG. 2. Kohler diagram of the transverse magnetoresistivity $\Delta\rho/\rho_0$ for the Al-Mn alloys as a function of B/ρ_0 .

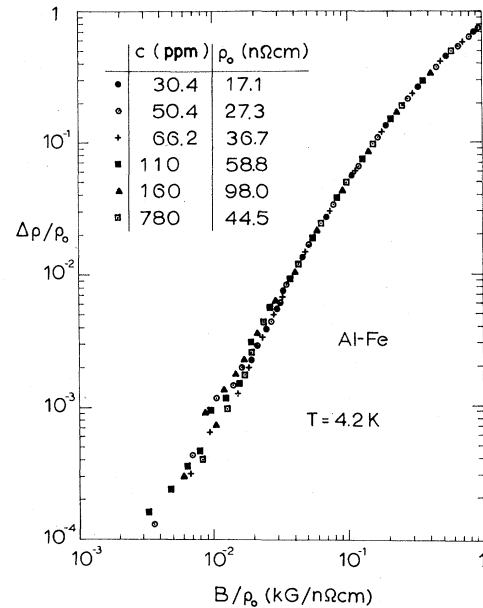


FIG. 3. Kohler diagram of the transverse magnetoresistivity $\Delta\rho/\rho_0$ for the Al-Fe alloys as a function of B/ρ_0 .

The Hall voltage and the transverse magnetoresistance measurements were performed at 4.2 K in a superconducting solenoid which produces a magnetic field up to 40 kG. Further experimental details have been described previously.¹⁰

III. EXPERIMENTAL RESULTS

Figures 1, 2, and 3 show the relative transverse magnetoresistivity $\Delta\rho/\rho_0$ of the Al-Cr, Al-Mn, and Al-Fe alloys, respectively, while Figs. 4, 5, and 6 show the Hall coefficient R_H . Both $\Delta\rho/\rho_0$

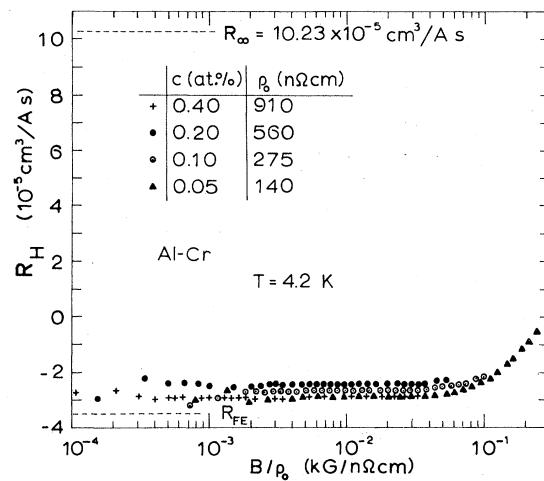


FIG. 4. Kohler plot of the low-field Hall coefficient R_H^0 as a function of B/ρ_0 for the Al-Cr alloys.

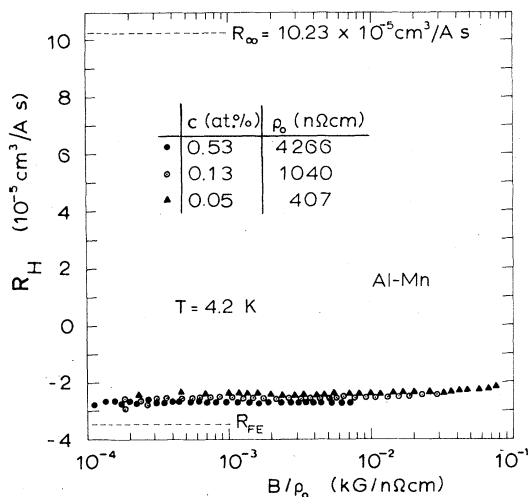


FIG. 5. Kohler plot of the low-field Hall coefficient R_H^0 as a function of B/ρ_0 for the Al-Mn alloys.

and R_H are represented in Kohler diagrams, i. e., are plotted as a function of the "effective" magnetic field B/ρ_0 , where ρ_0 is the residual resistivity of the specimens in zero magnetic field. In such a Kohler diagram various experimental curves should always fall upon each other when the scattering defects differ only in concentration but are of the same type and the Fermi surface remains unchanged. The inset tables on Figs. 1-6 show the values of the residual resistivity ρ_0 for the samples on which the Hall and magnetoresistance measurements were carried out. In the Al-Mn and Al-Fe alloys, ρ_0 at 4.2 K varied linearly with the solute concentration except for the Al-Fe specimen with 780-ppm Fe, which fell below the linear relationship. This exception is understandable because the maximum solubility of Al-Fe alloys is 180-ppm Fe.³ The residual resistivities per atomic percent in the present work are 8.1 $\mu\Omega$ cm/at. % for Al-Mn and 5.5 $\mu\Omega$ cm/at. % for Al-Fe respectively. These values are in good agreement with the values 8.05 $\mu\Omega$ cm/at. % for Al-Mn and 5.8 $\mu\Omega$ cm/at. % for Al-Fe obtained by Boato *et al.*³ The residual resistivity of the Al-Cr alloys also shows a linear dependence on the concentration of Cr impurities except for the specimen with the 0.40-at. % Cr. However, the residual resistivity per atomic percent was found to be about 2.8 $\mu\Omega$ cm/at. %, considerably lower than the previous values of 8.2,³ 8.4,¹¹ and 6.0 $\mu\Omega$ cm/at. %.⁹ This large discrepancy between the different experiments is for the moment inexplicable.

The measurements plotted in Figs. 1-6 show that the relative magnetoresistivity and the low-field Hall coefficient R_H^0 of the investigated alloys are practically independent of the impurity concen-

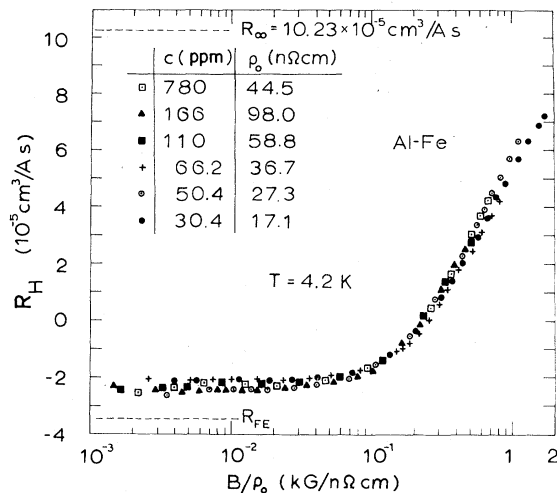


FIG. 6. Kohler plot of the low-field Hall coefficient R_H^0 as a function of B/ρ_0 for the Al-Fe alloys.

tration. The observed small deviations, especially in the low-field Hall coefficient R_H^0 , can be attributed to the errors in the determination of the thickness of the samples. In the low-field region in all alloys there is a very good quadratic relationship between $\Delta\rho/\rho_0$ and B/ρ_0 , while the Hall coefficients R_H^0 are constant and exhibit large negative values.

Table I shows the mean values of the low-field Hall coefficient R_H^0 at constant B/ρ_0 as well as ρ_0/c , of the present measurements, together with those of previous measurements. As shown in Table I, for the Al-Cr alloys there is a discrepancy in R_H^0 between the present investigation and that of McAlister *et al.*,⁹ while there is a very good agreement in R_H^0 for Al-Mn alloys between these two investigations. Note that the free-electron value for aluminum is $R_{FE} = -3.47 \times 10^{-5}$ cm³/A s.

The low-field Hall coefficient R_H^0 of the present measurements taken at a constant B/ρ_0 , together with values of the earlier investigations for Al-Cr,⁹ Al-Mn,⁹ and Al-Cu,¹⁰ are plotted in Fig. 7 as a function of the atomic number of the 3d impurity. It is seen from Fig. 7 that R_H^0 shows a distinct systematic dependence on the impurities, similar to those found in the residual resistivity, the thermopower and the superconducting transition temperature. R_H^0 becomes negative and even achieves the free-electron value when going from Cu impurities to Cr impurities in the 3d transition series.

IV. DISCUSSION

The low-field coefficients R_H^0 of the present Al-3d alloys are found to be always negative, tending

TABLE I. Low-field Hall coefficient R_H^0 and ρ_0/c .

Alloys	R_H^0 (10^{-5} cm ³ /A s)	ρ_0/c [$\mu\Omega$ cm/at. %]	Authors
Al-Cr	-2.75	2.8	This work
	-3.50	6.0	McAlister <i>et al.</i> ⁹
		8.2	Boato <i>et al.</i> ³
		8.4	Hamzic <i>et al.</i> ¹¹
Al-Mn	-2.65	8.1	This work
	-2.60	6.8	McAlister <i>et al.</i> ⁹
		8.05	Boato <i>et al.</i> ³
Al-Fe	-2.20	5.5	This work
		5.8	Boato <i>et al.</i> ³

towards the value R_{FE} when the 3d-impurity atoms vary from Fe to Cr.

In order to explain this behavior of R_H^0 we use the Friedel-Anderson model of the virtual 3d bound states^{1,2} together with the three-group model of the Fermi surface of Al. As mentioned in the introductory remarks, the 3d transitional elements when dissolved in Al form a VBS. This VBS is characterized by the distance ϵ_d of the free d state from the Fermi level and a half-width parameter Γ . Γ is related to the average s - d admixture matrix element $\langle V_{sd} \rangle$ and the electronic density of states $N_s(0)$ of the host conduction band at the Fermi level by

$$\Gamma = \pi N_s(0) |\langle V_{sd} \rangle|^2. \quad (1)$$

The VBS produces a change in the density of states per spin of Lorentzian form

$$N_d(\epsilon) = \frac{(2l+1)}{\pi} \frac{\Gamma}{(\epsilon - \epsilon_d)^2 + \Gamma^2}, \quad (2)$$

where $(2l+1)$ is the degeneracy of the d state.

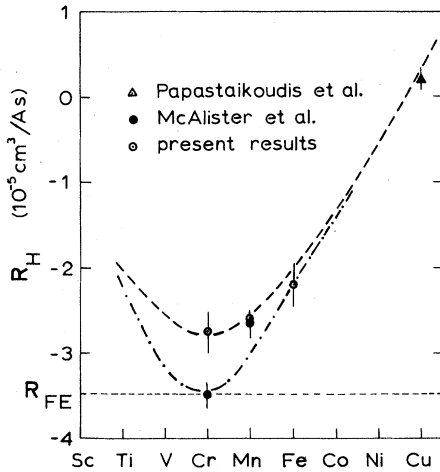


FIG. 7. The low-field Hall coefficient R_H^0 of aluminum alloys plotted versus atomic number of the impurity

For a nonmagnetic transition-element impurity dissolved in a normal host such as aluminum, the conduction-electron scattering consists of two components, namely, (i) a nonresonant scattering by the Coulomb potential of the impurity and (ii) a resonant scattering by the localized d states.^{3,12} The scattering events are assumed to be independent and thus the total relaxation time is written as a sum of a nonresonant and of a resonant part:

$$\tau_{\text{tot}}^{-1} = \tau_{\text{nr}}^{-1} + \tau_d^{-1}, \quad (3)$$

where τ_{nr} is due to the charge difference $Z_{\text{nr}} = Z_i - Z_h$ between the impurity and host atoms and τ_d is due to the charge Z_d . The charge Z_d is calculated by applying Friedel's sum rule¹ and assuming that the only significant phase shift η_l associated with the resonant scattering is that corresponding to the angular momentum $l=2$. The relaxation time τ_d for resonant scattering is given by³

$$\tau_d^{-1} = \frac{20c}{\pi\hbar N(\epsilon_F)} \sin^2 \eta_2 = \frac{20c}{\pi\hbar N(\epsilon_F)} \sin^2 \left(\frac{\pi Z_d}{10} \right), \quad (4)$$

where c is the impurity concentration and $N(\epsilon_F)$ is the density of states at the Fermi level.

Thus in the expression of the generalized Tsuji¹³ formula for the low-field Hall coefficient R_H^0 ,¹⁴

$$R_H^0 = - \frac{12\pi^3}{ec} \frac{\int_{\text{FS}} \langle 1/\kappa \rangle_{\text{av}} \tau^2(\vec{k}) v^2(\vec{k}) dS}{\left(\int_{\text{FS}} \tau(\vec{k}) v(\vec{k}) dS \right)^2}, \quad (5)$$

$\tau(\vec{k})$ is the sum of the nonresonant and resonant parts of the relaxation time, $v(\vec{k})$ is the electron velocity, and $\langle 1/\kappa \rangle_{\text{av}}$ is the mean value of the curvature of the Fermi surface (FS) at \vec{k} . The integration is carried out over the FS, dS being the surface element. The denominator is proportional to ρ_0^{-2} .

The systematic dependence of the low-field Hall coefficient R_H^0 in Al-3d alloys on the valence of the 3d impurities (Fig. 7) shows that the presence of the VBS causes the electronic mean free path $l_{\vec{k}}$

$=v_{\vec{k}} \cdot \tau_{\vec{k}}$ on the free-electron part of the FS to become predominant when going from Cu to Cr. The electron mean free path $l_{\vec{k}}$ depends on both the scattering potentials of the impurities present in the Al lattice, and on the electronic structure of the Al. Possible distortions of the aluminum FS due to the impurities can be rigorously excluded because of the validity of Kohler's rule.

The FS of aluminum can be divided into three regions S_{++} , S_{--} , and S_{-} (Refs. 14, 15, 16, and 17). The regions S_{++} and S_{--} are small areas near the intersecting Brillouin-zone boundaries, where the mean curvature $\langle 1/\kappa \rangle_{av}$ is very high and positive (strongly hole-like curvature in the second zone), and high and negative (strongly electron-like curvature in the third zone), respectively. These highly curved parts S_{++} and S_{--} can be approximated by cylinders. In the remaining spherical part S_{-} the mean curvature $\langle 1/\kappa \rangle_{av}$ is negative but its absolute value is about two orders-of-magnitude^{17,18} smaller than in S_{++} and S_{--} . Using this three-group model of conduction electrons of aluminum, Kesternich¹⁹ obtained simple formulas for $\Delta\rho/\rho_0$ and R_H^0 . In the nearly-free-electron (NFE) approximation $\Delta\rho/\rho_0$ and R_H^0 are given by

$$\frac{\Delta\rho}{\rho_0} = g_m \frac{\kappa_{FE}}{\kappa_L} \frac{l_{--}^3 + l_{++}^3}{2l_{-}^3} \left(\frac{R_{FE} B}{\rho_0} \right)^2 \quad (6)$$

and

$$R_H^0 = R_{FE} \left(1 + g_h \frac{l_{--}^2 - l_{++}^2}{2l_{-}^2} \right),$$

where l_{-} , l_{--} , and l_{++} are the respective free-electron-like, strongly electron-like and strongly hole-like mean free paths. κ_L and κ_{FE} are the radii of the cylindrical regions and of the free-electron sphere, respectively, and $R_{FE} = -3.47 \times 10^{-5} \text{ cm}^3/\text{Å s}$. For the geometry factors g_m and g_h Kesternich *et al.*¹⁶ have given the average values 3.0 and 3.75, respectively.

Using the above two equations of Kesternich,¹⁹ we have determined the mean-free-path values from the measurements of $\Delta\rho/\rho_0$ and R_H^0 , in terms of the ratios l_{++}/l_{-} and l_{--}/l_{-} , for the various concentrations of the Cr, Mn, and Fe atoms in the alloys.

Figures 8 and 9 show these ratios (right scale) for the currently investigated alloys, as well as the residual resistivity ρ_0 (left scale), as a function of Cr, Mn, and Fe concentrations. These are calculated for the fixed values of $B/\rho_0 = 0.02 \text{ kG/n}\Omega \text{ cm}$ (Al-Cr), $0.007 \text{ kG/n}\Omega \text{ cm}$ (Al-Mn), and $0.03 \text{ kG/n}\Omega \text{ cm}$ (Al-Fe) and for an average $\kappa_L = 0.03\kappa_{FE}$. These two figures show that $l_{++}/l_{-} \approx l_{--}/l_{-}$, i. e., $l_{++} \approx l_{--}$ for all investigated alloys. In the Al-Mn and Al-Fe alloys l_{++}/l_{-} and l_{--}/l_{-} are approximately equal to 1, while in Al-Cr they are < 1 .

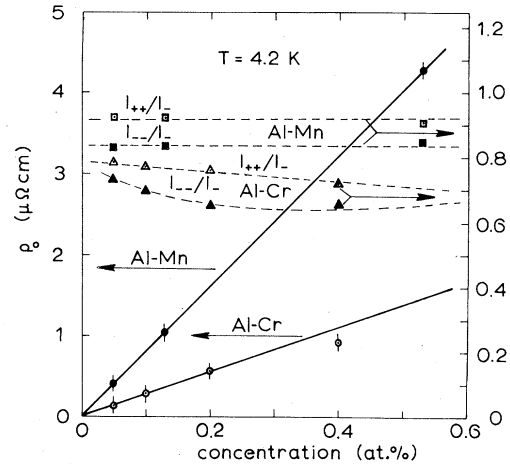


FIG. 8. The ratios of the mean free paths l_{++}/l_{-} and l_{--}/l_{-} and the residual resistivity ρ_0 , as a function of Cr and Mn concentrations.

However, the equality of l_{++} and l_{--} seems to contradict the arguments used for the analysis of the Hall data in Al alloys. These arguments are as follows: The wave function $\psi_{-}(\vec{r})$ on the spherical part of the FS is a plane wave, while $\psi_{++}(\vec{r})$ and $\psi_{--}(\vec{r})$ at the Brillouin-zone boundaries are standing waves. Böning *et al.*¹⁵ find from four orthogonalized plane-wave calculations that the amplitudes $|\psi_{--}(\vec{r})|^2$ and $|\psi_{++}(\vec{r})|^2$, which are proportional to the local charge densities $\rho_{\vec{k}}(\vec{r})$ of the electrons at the edges of the third- and second-zone states, are greatest at the lattice sites and

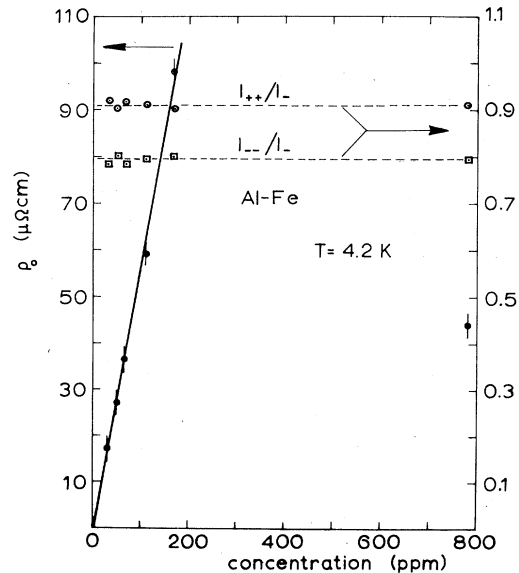


FIG. 9. The ratios of the mean free paths l_{++}/l_{-} and l_{--}/l_{-} and the residual resistivity ρ_0 , as a function of Fe concentration.

at the interstitial positions, respectively. The wave function $\psi_{\mathbf{k}}(\mathbf{r})$ has p -like character in the second zone and exhibits an s admixture in the third zone. Thus the electrons on the electron-like edges in the third zone will be scattered more strongly by a scattering potential centered at a lattice position, such as that from a substitutional defect, while the electrons on the hole-like edges in the second zone are affected most by an interstitial scattering potential. Electrons in states on the free-electron sphere are equally scattered by a substitutional or an interstitial potential. Thus it follows immediately from these arguments that the ratio l_{++}/l_- must be larger than l_{--}/l_- , i.e., $l_{++} \gg l_{--}$ for a substitutional defect.

In order to explain $l_{++} \approx l_{--}$ within the framework of these usual arguments, the simultaneous existence of an interstitial scattering potential must be assumed. McAlister *et al.*⁹ propose such an interstitial influence of the solutes Cr and Mn in Al to interpret their experimental results. They essentially ignore contributions from S_- and are able to obtain R_{FE} from the second-band alone. The "metallurgical" explanation of McAlister *et al.*⁹ seems rather unlikely to us since it has never been found that elements such as Cr or Mn occupy interstitial positions in metals such as Al. The mechanism proposed by the above authors is even more unlikely if the impurity atoms form extended clusters, where the concept of interstitially localized scattering centers becomes meaningless.

The currently investigated Al-Mn and Al-Fe alloys show a linear relationship between ρ_0 and the impurity concentration c , which is in good agreement with previous measurements,³ suggesting that Mn and Fe are randomly distributed substitutional defects. Therefore the mean-free-path inequality $l_{++} \gg l_{--}$ should hold true. The present measurements giving $l_{++} \approx l_{--}$ imply only one possibility, namely, the presence of an extra scattering mechanism which provides a compensating effect which eliminates this predicted inequality. This mechanism cannot arise from the metallurgical condition of alloys.

The distinct systematic dependence of R_H^0 on $3d$ solutes in Al (Fig. 7), being similar to that seen in the electrical resistivity,³ thermopower,⁴ and superconducting transition temperature,^{6,7} indicates that the extra scattering mechanism must be attributed to the existence of the $3d$ virtual bound state. Thus, as mentioned earlier, the electron scattering on a transition-element impurity in a normal host metal consists of two main parts, a nonresonant part due to the scattering of the electrons by the Coulomb potential of the impurity, and a resonant part due to their scattering by the localized d states.^{3,12} Thus, the total mean free

path l_{++} or l_{--} can be written as

$$(l_{\pm\pm})_{\text{tot}}^{-1} = (l_{\pm\pm})_{\text{nr}}^{-1} + (l_{\pm\pm})_d^{-1}. \quad (7)$$

The nonresonant part of the mean free path obeys the relation $(l_{++})_{\text{nr}} \gg (l_{--})_{\text{nr}}$ as already mentioned. Since the total mean free path satisfies $(l_{++})_{\text{tot}} \approx (l_{--})_{\text{tot}}$, it should be concluded from Eq. (7) that $(l_{++})_d \ll (l_{--})_d$, meaning that the VBS's scatter the electrons on the hole-like edges in the second zone more strongly than the electrons on the electron-like edges in the third zone.

In the spirit of the Friedel-Anderson model^{1,2} of the VBS and according to the above conclusion, i.e., $(l_{++})_d \ll (l_{--})_d$, we expect that the contribution of the hole-like edges in the second zone to the total scattering process increases as the VBS approaches the Fermi level of aluminum. This contribution must be largest for Cr and Mn atoms in the middle of the transition series, since the VBS associated with Cr and Mn impurities lie on the Fermi level of Al. Consequently these solutes should have the largest scattering probability for the electrons on the hole-like edges of the second zone.

According to the three-group model the variations of the low-field Hall coefficient [Eq. (6)] can be readily ascribed to differences in the scattering probabilities near the second- and third-zone Fermi surface edges. Therefore the observed systematic dependence of R_H^0 on the atomic d -occupation number and its large negative values for Cr and Mn impurities can be attributed to the increasing contribution of the second-zone FS edges to the total scattering event.

From the present measurements and those of McAlister *et al.*⁹ it can be seen that (i) in the Al-Fe alloys the sample of 780 ppm Fe, far above the solubility limit, gives the same R_H^0 value as the samples in the solid solution, and that (ii) in the Al-Mn system, used in both investigations, one obtains the same R_H^0 value, although the alloys have different ρ_0/c values. Furthermore, our alloys are in solid solution. All of this means that the low-field Hall coefficient R_H^0 is independent of any metallurgical condition of the alloys and thus provides extra evidence that the cause of such a behavior should be attributed to the VBS of the $3d$ elements. The discrepancy in the R_H^0 values observed in the Al-Cr alloys between the present measurements and those of McAlister *et al.*⁹ cannot be explained by the arguments presented above.

If the VBS model proposed here is correct, then the R_H^0 values of the rest of the Al-3d alloys should also lie on the curve of Fig. 7. A series of measurements on Al-Ti, Al-V, Al-Co, and Al-Ni alloys are in preparation in order to estab-

lish whether or not our proposed model is realistic.

V. CONCLUSION

We have reported measurements of the low-field Hall coefficient R_H^0 and the transverse magnetoresistivity for a series of Al-Cr, Al-Mn, and Al-Fe alloys at 4.2 K. The R_H^0 for these alloys takes unusually large negative values in comparison to other impurities in Al, and shows a systematic dependence on the atomic d -occupation number. A three-group model for the mean free path was used to explain the results. The free-

path ratios obtained seem to indicate that the resonance scattering of the $3d$ virtual bound state is playing the main role rather than the metallurgical condition of the alloys. Numerical values of the mean-free-path ratios l_{++}/l_- and l_{--}/l_+ as a function of the concentration of the Cr, Mn, and Fe atoms were computed from simultaneous Hall effect and magnetoresistance measurements.

ACKNOWLEDGMENTS

We thank Dr. Costas Papatriantafillou and Dr. Gregorios Papaioannou for careful reading of the manuscript.

¹J. Friedel, *Nuovo Cimento Suppl.* **7**, 287 (1958).

²P. W. Anderson, *Phys. Rev.* **124**, 41 (1961).

³G. Boato, M. Bugo, and C. Rizzuto, *Nuovo Cimento* **45**, 226 (1966).

⁴G. Boato and J. Vig, *Solid State Commun.* **5**, 649 (1967).

⁵R. Aoki and T. Ohtsuka, *J. Phys. Soc. Jpn.* **26**, 651 (1969).

⁶R. Aoki and T. Ohtsuka, *J. Phys. Soc. Jpn.* **23**, 955 (1967).

⁷E. Babic, P. J. Ford, C. Rizzuto, and E. Salamoni, *J. Low Temp. Phys.* **8**, 219 (1972).

⁸F. J. Kedves and L. Gergely, *Phys. Status Solidi A* **38**, K31 (1976).

⁹C. P. McAlister, C. M. Hurd, and L. R. Lupton, *J. Phys. F* **9**, 1849 (1979).

¹⁰C. Papastaikoudis, E. Thanou, D. Tsamakias, and

W. Tselfes, *J. Low Temp. Phys.* **34**, 429 (1979).

¹¹A. Hamzic, E. Babic, and B. Leontic, *Mater. Sci. Eng.* **23**, 271 (1976).

¹²B. E. Paton, *Can. J. Phys.* **49**, 1813 (1971).

¹³M. Tsuji, *J. Phys. Soc. Jpn.* **13**, 979 (1958).

¹⁴R. S. Sorbello, *J. Phys. F* **4**, 1665 (1974).

¹⁵K. Böning, K. Pfänder, P. Rosner, and M. Schlüter, *J. Phys. F* **5**, 1176 (1975).

¹⁶W. Kesternich, H. Ullmaier, and W. Schilling, *J. Phys. F* **6**, 1867 (1976).

¹⁷K. Pfänder, K. Böning, and W. Brenig, *Z. Phys. B* **32**, 287 (1979).

¹⁸K. Böning, K. Pfänder, P. Rosner, B. Lengeler, and J. M. Welter, *Z. Phys. B* **34**, 243 (1979).

¹⁹W. Kesternich, *Phys. Rev. B* **13**, 4227 (1976).